

# Magnetic Properties and Crystallization of Co-Pt Amorphous Metallic Alloys

Chung-Sik Yoo, Sung K. Lim, C. S. Yoon and C. K. Kim\*

Department of Materials Science and Engineering, Hanyang University, Seoul 133-781, Korea

(Received 16 June 2003)

$\text{Co}_{78-x}\text{Pt}_x\text{B}_{10}\text{Si}_{12}$  alloys were produced using the melt-spin process in order to study the crystallization behavior and ensuing magnetic properties of the  $\text{Co}_{78-x}\text{Pt}_x\text{B}_{10}\text{Si}_{12}$  (Co-Pt) amorphous alloys as a function of the Pt content. We showed that when  $x > 15$  well below its stoichiometric composition, CoPt crystallized in the amorphous alloy, thus greatly altering the crystallized microstructure and magnetic properties during annealing. Below this composition, the main crystallization product was Co with Pt dissolved in its lattice. In spite of the nucleation of CoPt with high magnetic anisotropy, the highest coercivity was obtained when  $x$  was 15. It was also concluded that the Pt addition deteriorated the glass stability, triggering the devitrification at a progressively lower temperature.

**Key words :** Amorphous metallic alloys, Crystallization, CoPt crystal, Anisotropy

## 1. Introduction

In the past decade, transition metal-metalloid amorphous magnetic alloys containing Fe, Ni, and Co have been intensively studied due to their soft magnetic properties ranging from low coercivities and hysteresis loss to high permeabilities, which render the alloys to be an outstanding candidate for host of applications including electronics, magnetic recording heads, magnetic sensors, and large transformers [1]. Most of all, material properties of these amorphous alloys were found to be sensitive to both composition and processing history, providing opportunities to tailor the magnetic and engineering properties of the material as desired. In addition to the practical applications, study of the amorphous alloy system provides important information on metastable glass structures and its crystallization kinetics as well as ensuing magnetic properties dictated by the microstructural evolution during the crystallization of the amorphous alloy.

Upon annealing, Co-based alloys were shown to develop a complex layered system involving cobalt oxide, crystalline cobalt and borosilicate depending on the temperature and annealing atmosphere, which had profound effects on the ensuing magnetic properties of the material [2-4]. In this study,  $\text{Co}_{78-x}\text{Pt}_x\text{B}_{10}\text{Si}_{12}$  amorphous alloys were produced in

order to see the effects of the Pt addition on the crystallization kinetics and magnetic properties. Although Co-Pt forms a complete solid solution, Pt addition slightly suppresses the liquidus temperature of the alloy near the Co-rich end of the phase diagram; hence, the solute addition should not affect the glass forming ability of the Co-amorphous alloy [5] while its large size and ability to form an intermetallic compound are expected to substantially alter the annealed microstructure and the resulting magnetic properties. Moreover, the Co-Pt alloy system has recently received much attention because of its high coercivity and magnetocrystalline anisotropy and its possible application in the high density magnetic recording media [6]. In this research we attempted to show that microstructure and crystallization kinetics of the  $\text{Co}_{78-x}\text{Pt}_x\text{B}_{10}\text{Si}_{12}$  amorphous alloys can provide information on the Pt solubility on crystalline Co crystallizing out of the metastable glass structure and its effect on the resulting microstructure and magnetic properties.

## 2. Experimental Details

Amorphous  $\text{Co}_{78-x}\text{Pt}_x\text{B}_{10}\text{Si}_{12}$  alloy strips were produced using the melt-spinning process. Typical samples produced were 20  $\mu\text{m}$  thick and 2 mm wide. Composition of the samples was verified with energy-dispersive X-ray spectroscopy and inductively-coupled plasma mass-spectroscopy.

Samples were annealed under vacuum ( $10^{-5}$  torr) for 50

\*Corresponding author: Tel: +82-2-2290-0409, e-mail: ckkim@hanyang.ac.kr

min. at temperatures ranging from 300 °C to 700 °C. Transmission electron microscopy (TEM) samples were prepared using an ion mill equipped liquid-nitrogen cooled cold stage to ensure minimal heating of the sample during milling. The electron microscopy was performed using JEM2000 and JEM2010 (JEOL, Japan). Powder X-ray diffractometer (XRD) (Rigaku, Rint-2000) using  $\text{CuK}\alpha$  radiation was used to identify the crystalline phase in the material and magnetic hysteresis loops were measured using a vibrating sample magnetometer (VSM) at room temperature.

### 3. Results and Discussion

Shown in Fig. 1 are the XRD patterns measured from the  $\text{Co}_{78-x}\text{Pt}_x\text{B}_{10}\text{Si}_{12}$  alloys annealed at different temperatures. As can be from the indexed diffraction pattern of the  $\text{Co}_{63}\text{Pt}_{15}\text{B}_{10}\text{Si}_{12}$  alloy in Fig. 1(a), the amorphous alloy devitrified predominantly through formation of Co crystallites with Pt dissolved in the Co lattice. Structural changes in the annealed amorphous alloy with  $x < 25$  was fully discussed elsewhere [7]. With  $x = 25$  and 39, Fig. 1 (b) and (c) show that the Pt content in the composition was high enough to nucleate the CoPt crystals well below the stoichiometric composition of CoPt. Judging from the XRD patterns, this transition composition, at which nucleation of CoPt becomes energetically favorable instead of forming a Co-Pt solid solution, lied between  $x = 15$  and  $x = 25$ . The CoPt phase formed in the amorphous matrix had a large effect on the subsequent crystallization path of the Co-Pt amorphous alloys. In the  $\text{Co}_{53}\text{Pt}_{25}\text{B}_{10}\text{Si}_{12}$  alloy, the final crystallization product mostly consisted of a mixture of ordered-CoPt and cobalt borides. A considerable fraction of  $\text{Co}_3\text{B}$  was initially observed after annealing the strip at 500 °C and the boride phase then decomposed into  $\text{Co}_2\text{B}$  and Co upon further heating. In comparison, the  $\text{Co}_{39}\text{Pt}_{39}\text{B}_{10}\text{Si}_{12}$  alloy initially crystallized into CoPt and FCC Co. A peak at 62.5°, which was not observed from the XRD patterns of other compositions appeared in the annealed  $\text{Co}_{39}\text{Pt}_{39}\text{B}_{10}\text{Si}_{12}$  alloy and its intensity became increasingly larger with increasing annealing temperature. The peak was tentatively matched to  $\text{Pt}_2\text{B}_3$  as no other relevant phases had a diffraction peak in the interval. Formation of  $\text{Pt}_2\text{B}_3$  was also observed in the XRD data of the annealed CoPt-B thin films [8]. The growth of the  $\text{Pt}_2\text{B}_3$  peak and decay of the CoB peak also suggest that CoB was gradually replaced by  $\text{Pt}_2\text{B}_3$  as the annealing temperature was increased. Since Pt-B compounds are thermodynamically more stable compared to Co-B compounds [8], the transformation from CoB to  $\text{Pt}_2\text{B}_3$  with increasing annealing temperature is quite plausible.

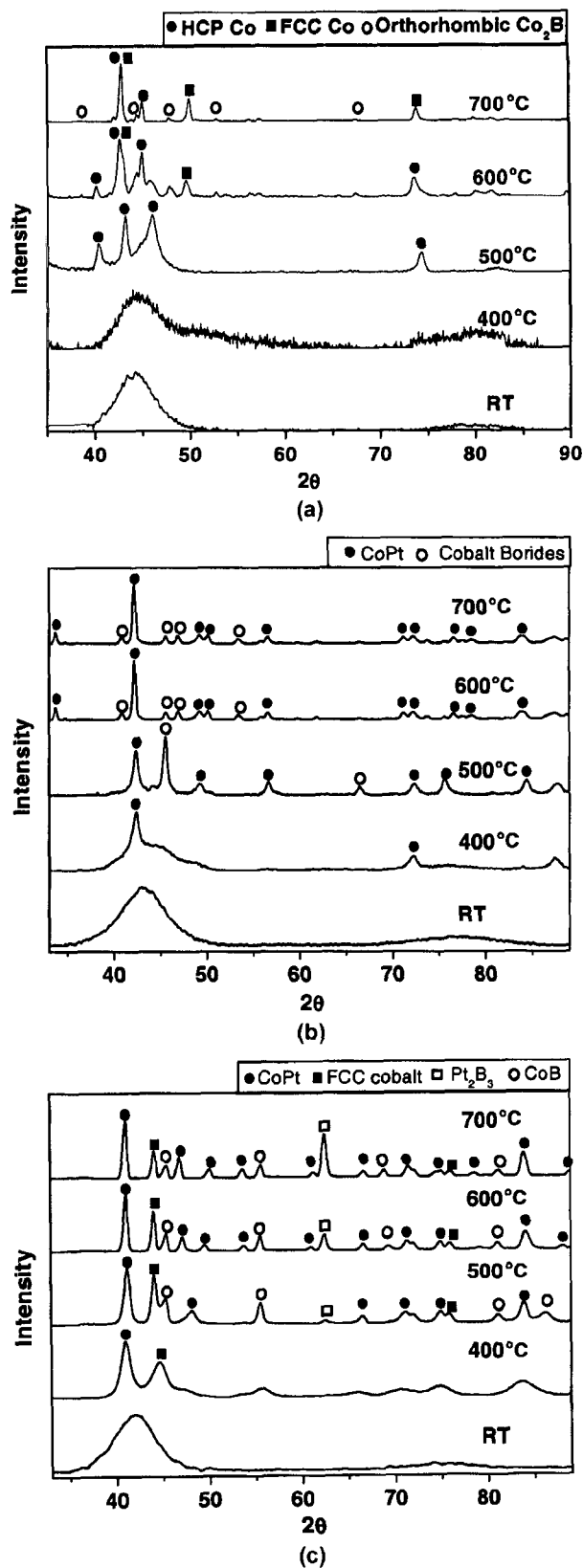


Fig. 1. XRD data for the thermally annealed amorphous alloy: (a)  $\text{Co}_{63}\text{Pt}_{15}\text{B}_{10}\text{Si}_{12}$ , (b)  $\text{Co}_{53}\text{Pt}_{25}\text{B}_{10}\text{Si}_{12}$ , (c)  $\text{Co}_{39}\text{Pt}_{39}\text{B}_{10}\text{Si}_{12}$  annealed at different temperatures.

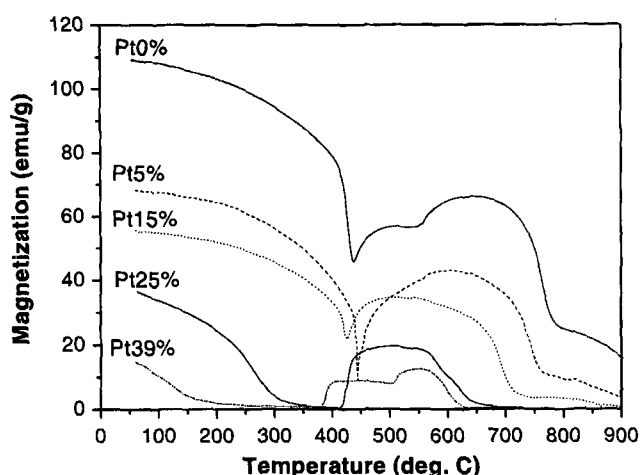


Fig. 2. In-situ measurement of magnetization at 5 KOe as a function of temperature for the  $\text{Co}_{78-x}\text{Pt}_x\text{B}_{10}\text{Si}_{12}$  amorphous alloys.

As seen from the XRD data, devitrification of the Co-Pt amorphous alloys was sensitive to the level of Pt addition, leading to a different set of final crystalline products depending on the Pt content. It was also observed that in agreement with the previous data [9], ordering of the CoPt phase into a  $L1_0$  structure occurred at 600 °C as evidenced by the splitted peaks at 50° (200 and 002) and 72° (220 and 202) in  $\text{Co}_{53}\text{Pt}_{25}\text{B}_{10}\text{Si}_{12}$ . In case of  $\text{Co}_{39}\text{Pt}_{39}\text{B}_{10}\text{Si}_{12}$ , the order-disorder transformation occurred at a slightly lower temperature.

In Fig. 2 the structural transition of the amorphous structure was further ascertained by the temperature dependence of the magnetization measured with applied field of 5 KOe that is well above the saturation magnetization. There was a sharp change in the Curie temperature,  $T_c$  of the amorphous alloy above  $x = 15$ . Below  $x = 15$ ,  $T_c$  was between 400 °C and 500 °C. As the Pt content was increased above  $x = 15$ ,  $T_c$  dropped sharply below 300 °C. Since  $T_c$  for CoPt is ~570 °C whereas  $T_c$  for pure Co is 1130 °C [10], above  $x = 15$ , the amorphous structure was

dominated by the Co-Pt bonds instead of Co-Co bonds so that its magnetic properties took on the characteristics of the crystalline CoPt in agreement with the XRD data. Increasing the Pt content also lowered the onset of the devitrification, defined in Fig. 2 as the temperature at which the value of the magnetization rose sharply due to the nucleation of the initial ferromagnetic crystalline phases. It is not clear why the onset of the devitrification should drop with the increasing Pt content. Since the nucleation and growth of crystalline phases in amorphous alloys are typically limited by the solid state diffusion and the presence of large solute atoms in the glass should retard the diffusion of relevant atoms [11], the Pt addition is expected to slow down the crystallization process. Instead, in contrast to the previous results for different metallic glass systems [12], we observed that in the Co-Pt amorphous alloys, Pt atoms destabilized the glass structure, resulting in the acceleration of the devitrification process.

Fig. 3 compares the crystallized microstructures of the amorphous alloys obtained using TEM. One unusual observation was that there was a large difference in grain size after annealing the  $\text{Co}_{39}\text{Pt}_{39}\text{B}_{10}\text{Si}_{12}$  and  $\text{Co}_{53}\text{Pt}_{25}\text{B}_{10}\text{Si}_{12}$  alloys at 400 °C and 500 °C. Comparing Fig. 3(a) and (b), the grain size went from being 10~30 nm at 400 °C to 200 nm 500 °C. The sudden grain growth was not observed in compositions with  $x < 15$ . Grain size in the Pt-rich compositions were, in general, larger than that of the Pt-depleted compositions as shown in Fig. 3(c). We cannot explain why there was a sudden grain growth at temperatures above 400 °C in the Pt-rich compositions, but it is speculated that in the crystallization of the Pt-rich compositions, the nucleation rate was sufficiently high that the grain impingement occurred at 400 °C which was followed by the grain coarsening at 500 °C. In case of compositions with  $x = 5$  and 15, it appears that there was relatively low density of nuclei at the onset of the crystallization so that initially nucleated crystallites were allowed to grow without the grain impingement; main-

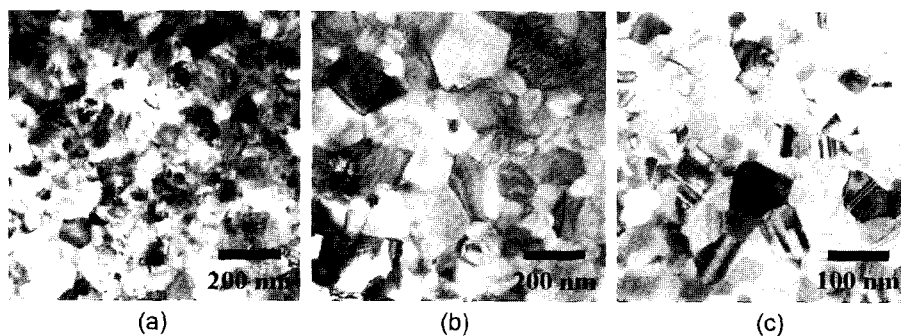


Fig. 3. TEM bright field images of the amorphous alloys: (a)  $\text{Co}_{39}\text{Pt}_{39}\text{B}_{10}\text{Si}_{12}$  annealed at 400 °C, (b)  $\text{Co}_{39}\text{Pt}_{39}\text{B}_{10}\text{Si}_{12}$  annealed at 500 °C, (c)  $\text{Co}_{63}\text{Pt}_{15}\text{B}_{10}\text{Si}_{12}$  annealed at 500 °C.

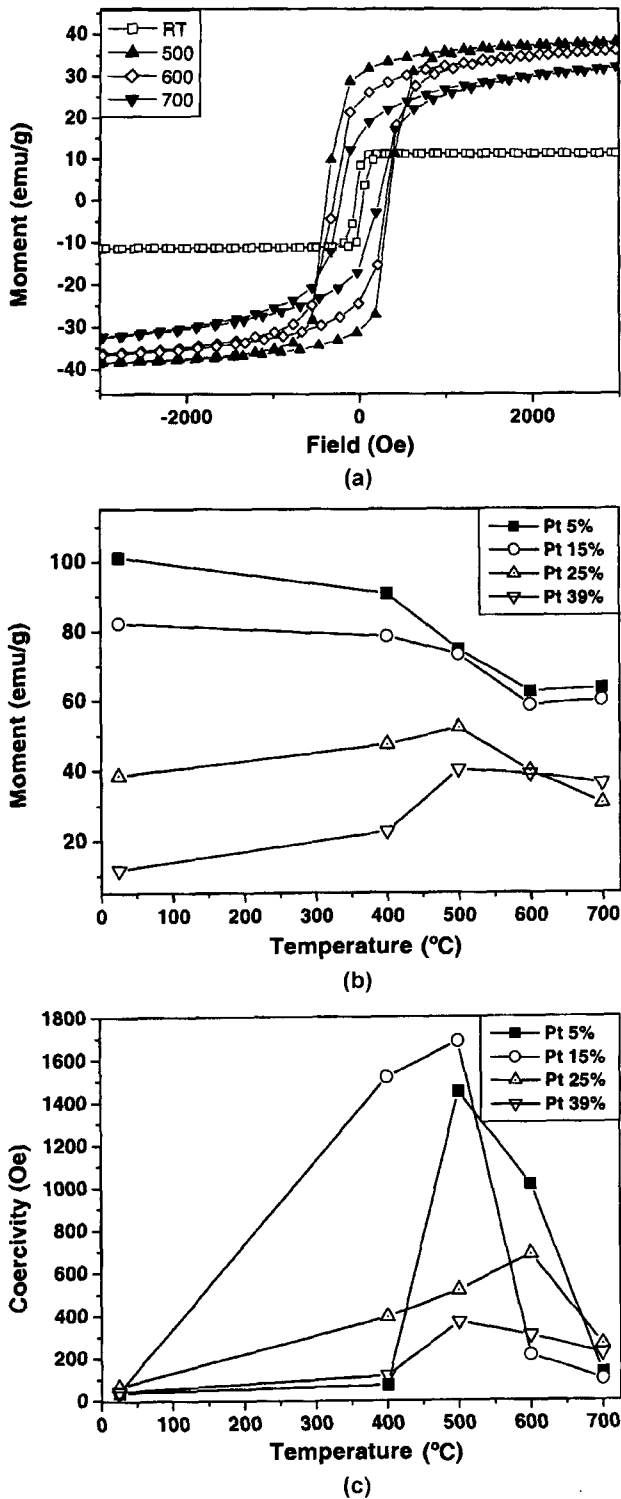


Fig. 4. (a) hysteresis loops for  $\text{Co}_{39}\text{Pt}_{39}\text{B}_{10}\text{Si}_{12}$  annealed at different temperatures, (b) saturation magnetization and (c) coercivity for the  $\text{Co}_{78-x}\text{Pt}_x\text{B}_{10}\text{Si}_{12}$  amorphous alloys annealed at different temperatures.

taining the relatively constant grain size during annealing. The fact that the Pt addition lowered the glass stability of

Co-Pt metallic glasses also supports the likely high rate of nucleation of crystallites in the Pt-rich glasses.

Fig. 4(a) shows a typical set of hysteresis loops obtained after annealing the  $\text{Co}_{39}\text{Pt}_{39}\text{B}_{10}\text{Si}_{12}$  alloy at different temperatures. Saturation magnetizations and coercivities of the  $\text{Co}_{78-x}\text{Pt}_x\text{B}_{10}\text{Si}_{12}$  alloys measured after annealing at different temperatures are summarized in Fig. 4(b) and (c). The saturation magnetization,  $M_s$  in Fig. 4(b) reflects two distinctively different crystallization paths depending on the Pt content. Below  $x = 15$ , the relatively high  $M_s$  value agrees with the presence of crystalline Co compared to the Pt-enriched compositions ( $M_s$  for pure CoPt = 54 emu/g,  $M_s$  for Co = 157 emu/g [10]).  $M_s$  of the alloys with  $x < 25$  decreased when heat treated due to the increased fraction of weakly ferromagnetic cobalt boride.  $M_s$  of the annealed strips for  $\text{Co}_{53}\text{Pt}_{25}\text{B}_{10}\text{Si}_{12}$  and  $\text{Co}_{39}\text{Pt}_{39}\text{B}_{10}\text{Si}_{12}$  rose slightly compared to the as-prepared amorphous strips in contrast to the compositions with the low Pt content. As can be seen from the coercivity data in Fig. 4(c), nucleation CoPt crystals reduced the coercivity of the annealed strips even though nucleation of CoPt with high magnetic anisotropy was expected to raise the coercivity of the crystallized alloy. We believe that the high coercivities of the  $\text{Co}_{73}\text{Pt}_5\text{B}_{10}\text{Si}_{12}$  and  $\text{Co}_{63}\text{Pt}_{15}\text{B}_{10}\text{Si}_{12}$  alloys were attributed to the high density of stacking faults within Co grains combined with the uniaxial anisotropy of HCP Co. It is possible that as CoPt became the dominant crystallization product, density of stacking faults proportionally decreased; thus, reducing sites where domain walls can be pinned.

#### 4. Conclusion

There was a sharp transition in the crystallization behavior of  $\text{Co}_{78-x}\text{Pt}_x\text{B}_{10}\text{Si}_{12}$  amorphous alloys depending the Pt content, chiefly due to the nucleation CoPt intermetallic compound in the Pt-rich compositions. The transition composition lied well below the stoichiometric composition (Co:Pt = 1:1). We also showed that the magnetic properties clearly correlated to the two distinctively different microstructural development observed with XRD and TEM. It was also observed that presence of Pt appeared to alter the as-prepared amorphous structure, destabilizing the glass structure and markedly reducing the Curie temperature. Further study is under-way to investigate the Pt effects on the amorphous structure of the Co-Pt amorphous alloys prior to devitrification.

#### Acknowledgment

This work was supported by the Korea Science and

Engineering Foundation through the Research Center for Advanced Magnetic Materials at Chungnam National University.

### References

- [1] F. E. Luborsky, in "Amorphous metallic alloys", edited by F. E. Luborsky, p 2 Butterworth & Co (Publishers) Ltd., (1983).
- [2] C. K. Kim, *Mat. Sci. & Eng.* **B34**, 1 (1995).
- [3] C. K. Kim, R. C. OHandley, *Metal. Mat. Trans. A* **28A**, 423 (1997).
- [4] C. K. Kim, C. S. Yoon, T. Y. Byun, and K. S. Hong, *Oxidation of Metals* **55**, 179 (2001).
- [5] E. A. Brandes, G. B. Brook (Editor), *Smithells Metals Reference Book*, p 11-200, Butterworth-Heinemann Ltd., Oxford (1992).
- [6] M. Jamet, M. Négrier, V. duuis, J. Tuailon-Combes, P. Mélinon, A. Pérez, W. Wernsdorfer, B. Barbara, and B. Baguenard, *J. Magn. Magn. Mater.* **237**, 293 (2001).
- [7] Chung-Sik Yoo, Sung K. Lim, C. S. Yoon, and C. K. Kim, accepted to *J. Alloys & Comp.* (2002).
- [8] H. Yamaguchi, O. Kitakami, S. Okamoto, Y. Shimada, K. Oikawa, and K. Fukamichi, *Appl. Phys. Lett.* **79**(13), 2001 (2001).
- [9] Q. F. Xiao, E. Bruck, Z. D. Zhang, F. R. de Boer, and K. H. J. Buschow, *J. Alloys & Comp.* **336**, 41 (2002).
- [10] H. P. J. Wijn (Editor), *Magnetic Properties of Metals: d-Elements, Alloys and Compounds* (Springer-Verlag, Berlin, 1991).
- [11] F. E. Luborsky, in "Amorphous metallic alloys", edited by F. E. Luborsky (Butterworth & Co (Publishers) Ltd., 1983).
- [12] J. L. Walter, *Mat. Sci. & Eng.* **50**, 137 (1981).